COMBINED NON-GRAY CONDUCTIVE AND RADIATIVE HEAT TRANSFER SIMULATION OF A SINGLE GLASS WINDOW SUBJECTED TO SOLAR AND THERMAL RADIATION

by

Maatouk KHOUKHI [a*] ***and Shigenao MARUYAMA*** [b]

[a] Department of Civil and Architectural Engineering, Sultan Qaboos University, Sultanate of Oman
[b] Institute of Fluid Science, Tohoku University, Sendai, Japan

Original scientific paper
DOI: 10.2298/TSCI130102142K

Combined non-gray conductive and radiative heat transfer in single glass window using the radiation element method by ray emission model REM2, has been investigated in one dimensional case. The optical constants of the glass window have been determined by using Fourier transform infrared spectrophotometer. The absorption and emission within the glass layer are taken into consideration. The boundary surfaces of the glass are specular. Spectral dependence of radiation properties of the glass is taken into account. Both collimated and diffuse solar and thermal irradiations are applied at boundary surfaces, using the spectral solar model proposed by Bird and Riordan. The simulation has been performed for one position of the Sun at noon true solar time on the 5th of July for three locations in Japan, Sendai, Tokyo, and Sapporo cities. Steady-state temperature and heat flux distributions within the glass layer for each position of the Sun of the three locations are obtained. The radiative heat flux through the glass mediums is the predominant mode compared with the conductive one. Therefore, the temperature distributions within the glass layer are not linear in shape.

Key words: *glass window, conduction, radiation, ray emission model, Fourier transform infrared spectrophotometer*

Introduction

Combined non-gray conductive and radiative heat transfer in single glass material has been investigated in one dimensional case using the radiation element method by ray emission model, (REM2). The REM2 is a generalized method for calculating radiation heat transfer between absorbing, emitting, and scattering media. The REM2 was proposed by Maruyama and Aihara [1] and can be applied for three dimensional complicated shapes. Heat transfer by combined conduction and radiation in glass medium has been reported by several references. Lee and Viskanta [2] have studied the combined heat transfer in glass medium in which the diffusion approximation and discrete ordinates method (DOM) are compared. The effect of the refractive index on radiative behavior of heated absorbing-emitting layer has been studied by Spuckler [3]. Extensive studies on the solar water collector assuming the glass cover as absorbing and emitting media subjected to solar and thermal radiation have been undertaken by Khoukhi and Maruyama [4, 6, 7] and Khoukhi *et al.* [5].

* Corresponding author; e-mail: mkhoukhi@squ.edu.om

In the present study an ordinary glass material is considered and the optical constants of the glass have been determined using Fourier transform infrared spectrophotometer (FTIR). Several techniques and experimental methods for determining the optical constants of glass material are given in [9]. Rubin has also determined the real part and the imaginary part, n and k, respectively, of the complex refractive index of clear absorbing and low-iron glasses using Kramers-Kroning (KK) formula [10]. This technique is very powerful in the range of strong absorption and consists to measure the reflectance of the sample at near-normal incidence. Hsieh and Su have also calculated the thermal radiative properties of glass from 0.32 to 206 m [11].

In the present work, the glass window is assumed to be a participating non-gray media subjected to solar radiation, specified by the spectral solar model proposed by Bird and Riordan [12], and thermal radiation specified by blackbody emission of the outside and inside environments. The boundary surfaces of the glass are specular and spectral dependence of radiative properties of such material is taken into consideration.

Steady-state temperature and heat flux distributions are obtained for three locations in Japan, Sendai, Tokyo and Sapporo. The calculation is performed on the 5th of July.

Procedure for determining the optical constants of a glass material

Experiment

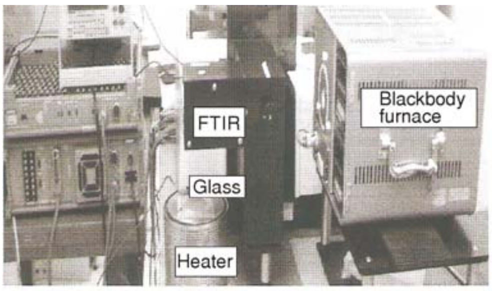

Figure 1. Arrangement of the experimental set-up

The measurement of the radiative properties of the glass material has been carried out using the Fourier transform spectrophotometer (FTIR-8001PC SHIMADZU), which is based on the Michelson interferometer principle. Figure 1 shows the arrangement of experimental set-up. First, we measured the blackbody radiation at 400 °C without the glass material, and then the glass is placed between the blackbody furnace and the FTIR zone detection. Finally, the measurement of the radiation that is transmitted or reflected by the glass material is performed. The temperature of the glass surface was measured by a T-type thermocouple soldered between dissimilar elements (copper and constantan, diameter = 0.076 mm). The diameter of the junction is 0.2 mm and the glass material thickness is 3 mm.

Method of calculation

The real and imaginary parts of the complex refractive index of the glass are given by the expressions [9]:

$$n = 0.5\left\{\frac{\left[\left(\dfrac{n_0}{\cos\theta}\right)^2 - (n_0\cos\theta)^2\right](R_s + R_p - R_s R_p - 1)}{(\mathrm{R}_s - R_p)\left(n_0\cos\theta + \dfrac{n_0}{\cos\theta}\right) + (1 - R_s R_p)\left(n_0\cos\theta - \dfrac{n_0}{\cos\theta}\right)}\right\} \tag{1}$$

$$k = \left\{ \frac{[R_s (n_0 \cos\theta + n)^2 - (n_0 \cos\theta - n)^2}{1 - R_s} \right\}^{0.5} \tag{2}$$

where n_0 is the refractive index of the air (= 1), θ – the angle of incidence. The R_p and R_s are the parallel and perpendicular polarised components, respectively. The FTIR-8001 cannot measure R_s and R_p separately, but those two components are related to the reflectance by the expression:

$$R = 0.5(R_s + R_p) \tag{3}$$

Moreover, when the incident angle is equal to 45°, the square of the perpendicular polarised component is equal to the parallel one, then:

$$R_s^2 = R_p \tag{4}$$

Combining eqs. (3) and (4), and solving the obtained equation of second order in R_s, we get the relation of R_s in term of the reflectivity R:

$$R_s = 0.5[-1 + (1 + 8R)^{0.5}] \tag{5}$$

Results

Since R can be measured by FTIR-8001, n and k values are computed using eqs. (1) and (2). The reflectivity curve in fig. 2 appears to be a function of n only at short wavelength, small around 0.05 and vary slowly in this range. At long wavelength the reflectivity has a large dependency on k. Figure 3 shows two major resonances centred around 9.5 μm and 21 μm.

The n and k values obtained with the measurement of the reflectivity at 45° by using eqs. 1 and 2 are in good agreement comparing with Rubin [10] and Hsieh and Su [11] data as shown by fig. 3. The slight difference is due essentially to the difference in colour and manufacturer. No precise values of n have been obtained in the visible and near infrared due to the noise from the measurement. On the other hand, the glass is almost transparent in the visible and near infrared ranges ($0.3 \leq \lambda \leq 4.6$ μm), this imply k is almost equal to zero.

Rubin [10] has determined with great precision the n values of the glass window in the visible and near infrared. A simplified form of dispersion equation proposed by Herzberger [10] fits his data to the third decimal.

$$n = 1.513 - 0.003169\lambda^2 + 0.003962\lambda^{-2} \tag{6}$$

The Herzberger model was used to calculate the real part of the complex refractive index in

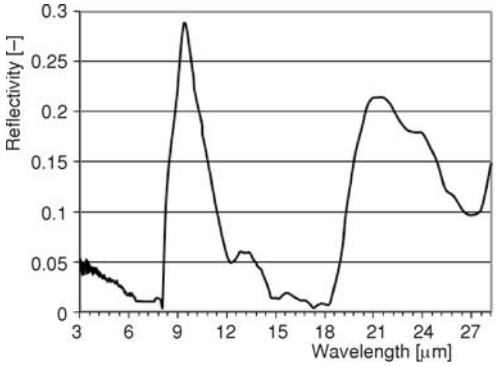

Figure 2. Reflectivity at 45°

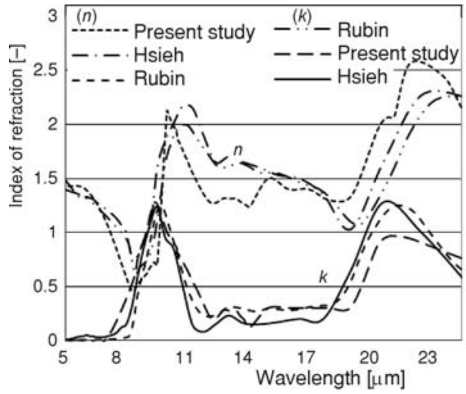

Figure 3. Variation of the optical constant of glass material

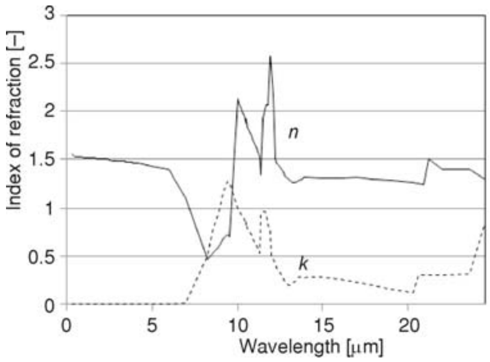

Figure 4. Real and imaginary parts of the complex refractive index of an ordinary glass material

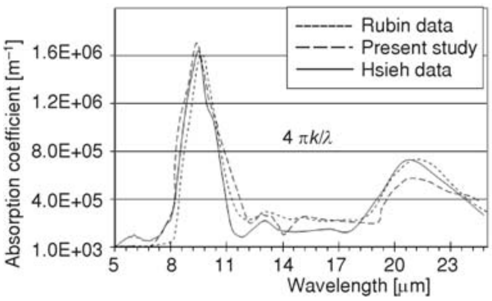

Figure 5. Absorption coefficient of an ordinary glass window

the range of interest (0.3 to 4.6 μm). In the short wavelength range where the glass is transparent, the extinction coefficient is small. Moving toward long wavelengths, the glass becomes opaque. The irregularity of *k* in the far infrared is associated with the molecular vibration [11]. Indeed, the extinction coefficient curve shows two ranges of strong absorption of the glass at about 9 and 20 μm, which can be ascribed to Si-O-Si stretching and rocking vibration [11]. Weak absorption bands are also present at about 13 and 16 μm and have been assigned to vibrations which combine rocking and stretching or to vibrations of silicon-oxygen ring structure [11]. Figure 4 shows the variation of the real (*n*) and imaginary (*k*) parts of the complex refractive index of an ordinary glass material after adjusting the value of *n* by using the Herzberger model.

The absorption coefficient of the glass is plotted in fig. 5. The general shape fits the absorption coefficients obtained using Rubin [10] and Hsieh and Su [11] data. The magnitude of the absorption coefficient obtained in this present study around 21 μm is slightly smaller comparing with those obtained by Rubin and Hsieh data.

Model analysis of the glass window

Assumptions and data used in numerical simulation

Figure 6 shows the glass window subjected to internal and external thermal radiation and external solar radiation (collimated and diffuse solar and thermal irradiations). The glass is considered as a non-gray medium and discretized into 103 elements layers. Each element is assumed at constant temperature as shown by fig. 7. Since the long-wavelength radiation from the

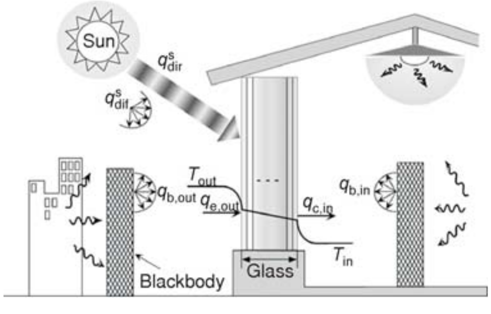

Figure 6. Glass window subjected to solar and thermal radiations

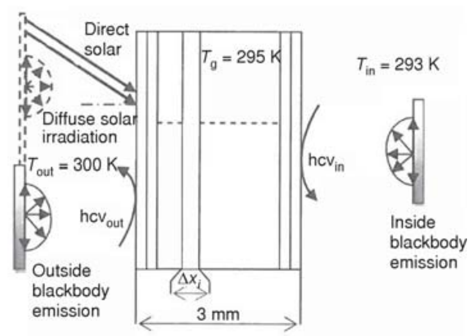

Figure 7. Analysis model of glass window

ambient is mostly absorbed in the vicinity of the glass surface, the thickness of the element is thin (1 μm) at the glass surface and thick (200 μm) in the middle of the glass. The refractive index and heat generation per unit volume are also constant over each radiation element. The thermal conductivity of the glass is constant and spectral independency is considered. The simulation has been performed for one position of the Sun at noon true solar time for each location on the 5th of July and the zenith angle is calculated for each case.

Table 1. Analytical data

Parameters	Values
T_g	295 K
T_{out}	300 K
T_{in}	293 K
Za	Sendai: 15.43° Tokyo: 13° Sapporo: 20.27°

Tables 1, 2, and 3 give the analytical data, thermo physical properties of the glass and the geographical data for each site, respectively.

Table 2. Thermophysical properties of glass window

Parameters	Values
λ	1 [Wm^{-1}K^{-1}]
ρ	2600 [kgm^{-3}]
c_p	600 [Jkg^{-1}K^{-1}]

Table 3. Geographical data of sites

Sites	Altitude	Latitude	Longitude
Sendai	45 m	38.16°	140.51°
Tokyo	0	35.65°	139.74°
Sapporo	0	43.03°	141.21°

The ground albedo is assumed to be equal to 0.2 for the three locations.

Basic equations

Under accepted assumptions and using the direction cosine of each ray the radiation intensity for participating media is given by [1]:

$$\mu \frac{\mathrm{d}i_\lambda(x,\mu)}{\mathrm{d}x} = \kappa_\lambda[-i_\lambda(x,\mu) + i_{\lambda,\mathrm{b}}(T)] \tag{7}$$

The solution of the equation is:

$$i_\lambda(x+\Delta x_i,\mu) = i_{\mathrm{b},\lambda}(T)\left[1-\exp\left(\frac{-\kappa_\lambda \Delta x_i}{\mu}\right)\right] \tag{8}$$

The radiant energy emitted from the element i can be approximated as:

$$\mathrm{d}Q_{\mathrm{J},i,\lambda} = i_{\mathrm{b},\lambda}\mu\left[1-\exp\left(\frac{-\kappa_\lambda \Delta x_i}{\mu_\mathrm{k}}\right)\right]\mathrm{d}w \tag{9}$$

Integrating over all solid angles, the spectral radiation energy from the radiation elements i is given by:

$$Q_{\mathrm{J},i,\lambda} = i_{\mathrm{b},\lambda}\sum_{k=1}^{K}\mu_\mathrm{k}\left[1-\exp\left(\frac{-\kappa_\lambda \Delta x_i}{\mu_\mathrm{k}}\right)\right]w_\mathrm{k} \tag{10}$$

The effective area is given by the expression:

$$A_i^R = \frac{1}{\pi}\sum_{k=1}^{K}\mu_\mathrm{k}\left[1-\exp\left(\frac{-\kappa_\lambda \Delta x_i}{\mu_\mathrm{k}}\right)\right]w_\mathrm{k} \tag{11}$$

The rate of spectral radiation energy emitted by the radiation element can be expressed in generalized form:

$$Q_{J,i,\lambda} = A_i^R \varepsilon_i n^2 \sigma T^4 \tag{12}$$

where ε_i, n, σ, and T are the emissivity of the glass, real part of the complex refractive index of the glass, Steffan Boltzman constant, and temperature, respectively.

The net rate of heat generation can be derived from the heat balance on the radiation element:

$$Q_{X,i,\lambda} = A_i^R \varepsilon_i (n^2 \sigma T^4 - G_{i,\lambda}) \tag{13}$$

The expressions of heat transfer rates of irradiation energy $Q_{G,i,\lambda}$ and emissive power $Q_{T,i,\lambda}$ of the radiation element are:

$$Q_{G,i,\lambda} = A_i^R G_{i,\lambda} \quad \text{and} \quad Q_{T,i,\lambda} = A_i^R \varepsilon_i n^2 \sigma T^4 \tag{14}$$

If the system is consisted of N volume and surface elements, then:

$$Q_{J,i,\lambda} = Q_{T,i,\lambda} \tag{15}$$

$$Q_{X,i,\lambda} = Q_{T,i,\lambda} - \sum_{j=1}^{N} F_{j,i}^A Q_{J,j,\lambda} \tag{16}$$

in which, the absorption view factor is introduced as defined by Maruyama and Aihara [1]. The heat transfer rate of spectral emissive power $Q_{T,i,\lambda}$ or the net rate of heat generation $Q_{X,i,\lambda}$ for each radiation element is given arbitrary as a boundary conditions. The convection is taken into consideration as boundary conditions in both side of the glass. The outside convective heat transfer coefficient is given by the following equation [13].

$$hcv_{out} = 5.7 + 3.8V \tag{17}$$

where V is the wind speed.

The inside convective heat transfer coefficient is determined by the classical equations, assuming the natural convection of the air and given by:

$$\text{Gr} = \frac{g|T_{in} - T_g|}{\nu^2 T_{in}} \tag{18}$$

$$\text{Nu} = 0.56(\text{Ra})^{0.25} \quad \text{and} \quad \text{Ra} = \text{Gr Pr} \tag{19}$$

$$hcv_{in} = \frac{\text{Nu}\lambda_{air}}{H} \tag{20}$$

where Gr, Nu, and Ra are the Grashoff, Nusselt and Rayleigh numbers, respectively. The λ_{air} and ν are the thermal conductivity and the kinematic viscosity of the air, respectively.

The unsteady one dimensional conductive heat transfer through the glass layer is given by:

$$\rho c_p \frac{\partial T}{\partial t} = \lambda_g \frac{\partial T^2}{\partial x^2} + S_h \tag{21}$$

where ρ, c_p, λ_g, t, and S_h are the density, specific heat, thermal conductivity, time and source, respectively.

Spectral solar model

The direct irradiance on a surface normal to the direction of the sun at ground level for wavelength λ is given by the expression [12]:

$$I_{d\lambda} = H_{o\lambda} D T_{r\lambda} T_{a\lambda} T_{w\lambda} T_{o\lambda} T_{u\lambda} \tag{22}$$

where $H_{o\lambda}$ is the extraterrestrial irradiance, D – the correction factor for the earth-sun distance, and $T_{r\lambda}$, $T_{a\lambda}$, $T_{w\lambda}$, $T_{o\lambda}$, and $T_{u\lambda}$ are the Rayleigh scattering, aerosol attenuation, water vapour absorption, ozone absorption, and uniformly mixed gas absorption, respectively.

The spectral global irradiance on an inclined surface is given by:

$$I_{T\lambda} = I_{d\lambda}\cos\theta + I_{s\lambda}\left\{\frac{I_{d\lambda}\cos\theta}{H_{o\lambda}D\cos Z} + 0.5\left[1+\cos t\left(1-\frac{I_{d\lambda}}{H_{o\lambda}D}\right)\right]\right\} + 0.5 I_{T\lambda} r_{g\lambda}(1-\cos t) \quad (23)$$

where θ is the angle of incidence of the direct beam on the tilted surface, t the tilt angle and $r_{g\lambda}$ is the spectral albedo of the ground. The $I_{T\lambda}$ is the global irradiance on horizontal surface given by the relation:

$$I_{T\lambda} = I_{d\lambda}\cos Z + I_{s\lambda} \quad (24)$$

Results and discussion

The simulation has been carried out using the real and the imaginary parts of the complex refractive index of the glass material as shown in fig. 4. However, the CPU time consumed was found to be prohibitively long on personal computer (VT-Alpha 600, 21164 A, 600 MHz). Therefore, a simplified non-gray model with 10 values of n and k has been used for quick simulation. The proposed model has been already validated in the previous works [5]. The model with 10 bands is shown by fig. 8. One can see that the curve of the real part of the complex refractive index n shows two picks around 11 and 21 μm, and the curve of the imaginary part k shows two bands of strong absorption around 9 and 21 μm similar to what it has been described in fig. 4.

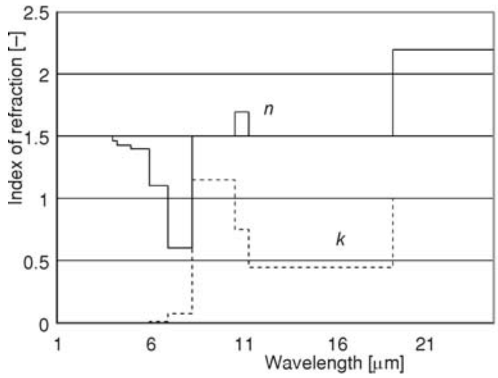

Figure 8. Real part (*n*) and imaginary part (*k*) of the complex index of refraction of glass window (10 bands model)

The temperature and heat flux distributions in glass medium are given by figs. 9 and 10, respectively. One can see that the effect of the radiative heat transfer is very important compared with the heat transfer due to the conduction alone. This is due essentially to the small gradient of the temperature between the inside and outside room (7°C). Consequently, the profiles of the temperature distribution within the glass layer are not linear in shape. The temperature distribution within the glass layer obtained in this present study is higher in case of Sapporo site compared with Sendai and Tokyo locations. Therefore, the heat flux within a glass medium is higher and found to be equal to 346 W/m^2 for this site.

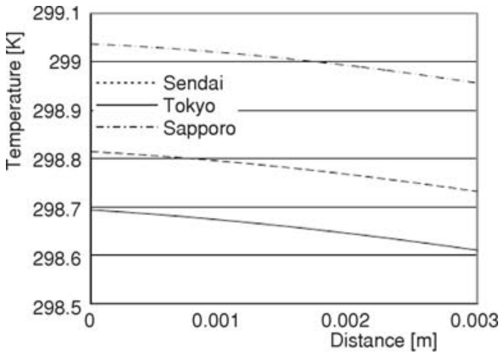

Figure 9. Temperature distributions in glass medium

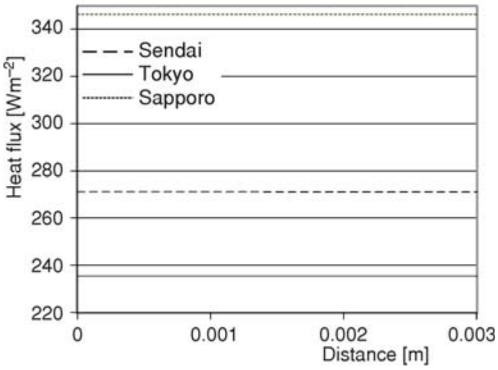

Figure 10. Heat flux distribution in glass medium

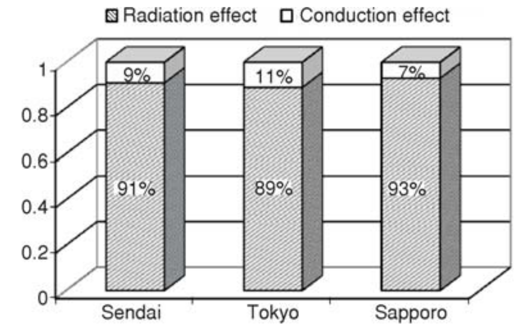

Figure 11. Conductive and radiative heat transfer effects on the glass window material

Figure 11 shows the conductive and radiative heat transfer effect on the glass window material. As it was mentioned before, the radiation mode is the predominant one. The ratio of the heat flux by conduction to the overall heat flux (conduction + radiation) is lower than 11 % for the three sites.

Conclusions

Thermal behavior of an absorbing-emitting glass window subjected to solar and thermal infrared irradiation, using the radiation element method, by ray emission model in one dimensional case has been presented. Both collimated and diffuse solar and thermal irradiations are applied at boundary surfaces, using the spectral solar model proposed by Bird and Riordan [12].

The computation has been performed using the model of the complex refractive index of the glass obtained by using FTIR combined with Rubin [10] data. The CPU time was found to be prohibitively long. Therefore, a non-gray model with ten bands has been proposed for rapid simulation.

The effect of the radiation and conduction heat fluxes on the overall heat flux is examined. The shape of the temperature distribution within the glass layer depends essentially on the predominant heat transfer mode. The temperature distributions also are affected by the real and imaginary parts of the complex refractive index of the glass. Indeed, the profiles of the temperatures were found to be not linear in shape due to the strong effect of the radiation on the overall heat transfer.

Nomenclature

A_i^R – effective radiation area, [m^2]
$F_{i,j}^A$ – absorption view factor from element *i* to *j*
$G_{i,\lambda}$ – incident radiation, [Wm^{-2}]
H – height of the glass (= 1 m)
hcv_{in} – convective heat transfer coefficient, [Wm^{-2}K^{-1}]
i_λ – radiation intensity, [Wm^{-2}μm^{-1}sr^{-1}]
$i_{\lambda \mathrm{b}}$ – blackbody radiation intensity, [Wm^{-2}μm^{-1}sr^{-1}]
I_{sl} – total scattering irradiance, [Wm^{-2}μm^{-1}sr^{-1}]
n – refractive index of element i of glass layer
$Q_{J,i,\lambda}$ – heat transfer rate of diffuse radiosity, [W]
$Q_{T,i,\lambda}$ – heat transfer rate of emissive power, [W]
$Q_{x,i,\lambda}$ – net heat transfer rate of heat generation, [W]
$q_{r,\lambda}$ – radiative heat flux, [Wm^{-2}]
$q_{x,i}$ – net rate of heat generation per unit volume or unit surface [Wm^{-3}, Wm^{-2}]
T – temperature [K]
$T_{r\lambda}$ – Rayleigh scattering, [Wm^{-2}μm^{-1}sr^{-1}]
$T_{a\lambda}$ – aerosol attenuation, [Wm^{-2}μm^{-1}sr^{-1}]
$T_{w\lambda}$ – water vapour absorption, [Wm^{-2}μm^{-1}sr^{-1}]
$T_{o\lambda}$ – ozone absorption, [Wm^{-2}μm^{-1}sr^{-1}]

$T_{u\lambda}$ – uniformly mixed gas absorption, [$Wm^{-2}\mu m^{-1}sr^{-1}$]
V – wind speed, [ms^{-1}]

Greek symbols

Δ_{xi} – element thickness, [m]
ε_i – emissivity, [–]
κ_λ – absorption coefficient, [m^{-1}]
λ_{air} – conductivity of air [$Wm^{-1}K^{-1}$]
μ – direction cosine of polar angle
ν – kinematic viscosity, [m^2s^{-1}]
w_k – solid angle

References

[1] Maruyama, S., Aihara T., Radiation Heat Transfer of Arbitrary Three Dimensional Absorbing Emitting and Scattering Media and Specular and Diffuse Surfaces, *Journal of Heat Transfer, 119* (1997), 1, pp. 129-136
[2] Lee, K. H., Viskanta, R., Comparison of the Diffusion Approximation and the Discrete Ordinates Method for the Investigation of Heat Transfer in Glass, *Glastech. Ber. Glass Sci. Technol, 72* (1999), 8, pp. 254-265
[3] Spuckler, C. M., Siegel, R., Refractive Index Effects on Radiation Behaviour of Heated Absorbing-Emitting Layer, *Journal of Thermophysics and Heat Transfer, 6* (1992), 4, pp. 596-604
[4] Khoukhi, M., Maruyama, S., Temperature and Heat Flux Distribution through Single and Double Window Glazing Nongray Calculation, *Smart Grid and Renewable Energy, 2* (2011), 1, pp. 21-26
[5] Khoukhi, M., *et al.*, Combined non Gray Radiative and Conductive heat Transfer in Solar Water Collector Glazing, *Solar Energy, 75* (2003), 4, pp. 285-293
[6] Khoukhi, M., Maruyama, S., Theoretical Approach of Flat-plate Solar Collector with Clear and Low-iron Glass Covers Taking into Account the Absorption and Emission within Glass Covers Layer, *Renewable Energy, 30* (2005), 8, pp. 1177-1194
[7] Khoukhi, M., Maruyama, S., Theoretical Approach of Flat-plate Solar Collector Taking into Account the Absorption and Emission within Glass Cover Layer, *Solar Energy, 80* (2006), 7, pp. 787-794
[8] Khoukhi, M., Non-Gray Radiative and Conductive Heat Transfer in Single and Double Glazing Solar Collector Glass Covers, *International Journal of Thermal Sciences, 45* (2006), 6, pp. 579-585
[9] Ward, L., *The Optical Constants of Bulk Materials and Films*, Taylor and Francis, Washington D.C., 1998
[10] Rubin, M., Optical Properties of Soda Lime Silica Glasses, *Solar Energy Materials, 12* (1985), 4, pp. 275-288
[11] Hsieh, C. K., Su, K. C., Thermal Radiative Properties of Glass from 0.32 to 206 m, *Solar Energy, 22* (1978), 1, pp. 37-43
[12] Bird, R. E., Riordan, C., Simple Solar Spectral Model for Direct and Diffuse Irradiance on Horizontal and Tilted Planes at the Earth's Surface for Cloudless Atmospheres, *American Meteorological Society, 25* (1986), 1, pp. 87-97
[13] Duffie, J. A., Beckman, W. A., *Solar Energy Thermal Process*, John Wiley & Sons, New York, USA, 1974

Paper submitted: January 2, 2013
Paper revised: October 10, 2013
Paper accepted: October 15, 2013